

# A Fast Radiative Transfer Model for AMSU-A Channel-14 with the Inclusion of Zeeman-splitting Effect

Yong Han

NOAA/NESDIS/Center for Satellite Applications and Research  
5200 Auth Road, Camp Springs, MD 20746, USA

## Abstract

AMSU-A channel 14 has four narrow passbands, centered on the sides of the 11- (57.6125 GHz) and 13- (56.9682 GHz) O<sub>2</sub> magnetic dipole transition lines, and the sensitivity of the channel peaks around 40 km. Because of the Zeeman-splitting, the radiances are partially polarized and dependent on the Earth's magnetic field and its orientation with respect to the observation direction. So far, the Zeeman-splitting effect has either not been taken into account or incorrectly modelled in the radiative transfer scheme applied for radiance assimilations. The work reported here is an attempt to model the Zeeman-splitting effect as part of the development of the Community Radiative Transfer Model (CRTM).

## Introduction

Zeeman splitting has a small, but non-negligible effect on AMSU-A channel 14. This paper describes a fast radiative transfer model that takes the Zeeman effect into account for this channel and introduces a way to derive from the AMSU-A 1B data stream the parameters which are required as the model inputs. The first section provides a description about the Zeeman effect on the channel, followed by a section describing the model algorithm. The next section presents procedures for obtaining the model inputs from the 1B data stream. The last section summarizes the results.

## Effect of Zeeman-splitting on AMSU-A channel 14

In the 60 GHz frequency region, there is a cluster of O<sub>2</sub> magnetic dipole transition lines. These lines are usually designated as the  $N^+$  and  $N^-$  lines, representing respectively the transitions between the  $J = N$  and  $J = N + 1$  and between  $J = N$  and  $J = N - 1$  energy levels, where  $J$  is the quantum number of the total angular momentum and  $N$  (an odd number) is the quantum number of the rotational angular momentum. In the upper stratosphere and mesosphere, the lines become sharp and a phenomenon called the Zeeman effect appears, induced by the interaction of the O<sub>2</sub> molecule's magnetic dipole moment with the earth's magnetic field. The energy level  $J$  splits into  $2J + 1$  new levels, associated with the azimuth quantum number  $M$ , which may take any integer number from  $-J$  to  $J$ . The selection rules permit the  $N^+$  and  $N^-$  transitions for which the  $M$  number can either remain fixed or change by one. Thus, each of the  $N^+$  and  $N^-$  lines splits into three groups of sublines. The line components obtained when  $M$  is unchanged are called the  $\pi$  components. When  $M$  increases or decreases by one, the components are called the  $\sigma^+$  or  $\sigma^-$  components.

The three groups of components show different behaviours in polarization. The  $\pi$  components are linearly polarized in the direction perpendicular to the plane containing the magnetic field vector  $\mathbf{Be}$  and the wave propagation direction  $\mathbf{k}$ . Their magnitudes reach a maximum when the angle  $\theta_{Be}$  between  $\mathbf{Be}$  and  $\mathbf{k}$  is  $90^\circ$  and become zero when the angle is zero. The  $\sigma^+$  and  $\sigma^-$  components are respectively right and left circularly polarized when  $\mathbf{Be}$  and  $\mathbf{k}$  point in the same direction ( $\theta_{Be} = 0^\circ$ ) and exchange the polarizations when  $\mathbf{Be}$  and  $\mathbf{k}$  point in the opposite direction ( $\theta_{Be} = 180^\circ$ ). They become linearly polarized at  $\theta_{Be} = 90^\circ$  in the plane containing  $\mathbf{Be}$  and  $\mathbf{k}$ . When the angle  $\theta_{Be}$  takes other values, the polarization of the  $\sigma^+$  and  $\sigma^-$  components are elliptical. The total splitting width (the spread range of the sublines) is about  $0.5Be$  MHz, where  $Be$  is the strength of the earth's magnetic field, which may take a value in the range of 0.23 – 0.65 in Gauss unit near the earth surface. Thus,

the Zeeman effect can only be observed by sensors with very narrow passbands on or near the centers of the unsplit  $N+$  and  $N-$  lines and their sensitivity peak in the upper stratosphere and mesosphere.

AMSU-A channel 14 has four passbands, 4.5 MHz away from the centers of the transition lines 11- and 13- with bandwidths of 2.9 MHz. Its sensitivity peaks around 40 km as shown in Figure 1. The impact of the Zeeman effect on this channel is revealed by a slight shift of the weighting function upward when the magnetic field strength  $Be$  increases. The impact is also illustrated in Figure 2, which shows its dependence on  $Be$ ,  $\theta_{Be}$  and the orientation of the receiver's polarization. As the figure shows, in theory it can have an impact up to 1K. However, in reality, the combination of the AMSU-A observation geometry and the orientation of  $Be$ , shown in Figure 3A and 3B, does not provide the conditions for the maximum impact to happen, as shown in Figure 3C. In these figures, the global distributions of the  $Be$  and  $\cos(\theta_{Be})$  parameters on the AMSU-A pixels are computed from the data in the 1B data stream. Figure 3C shows the difference between simulated brightness temperatures with and without the inclusion of Zeeman effect. The variations of the receiver's polarization due to scanning have been taken into account. It can be seen that in the low latitude regions, although  $\theta_{Be}$  can reach a value of  $90^\circ$ , a condition for the maximum impact, the  $Be$  value is generally low, resulting in a relatively small impact. On the other hand, in the regions in which  $Be$  has large values (around 0.65 Gauss), the  $Be$  vector is near parallel with the  $\mathbf{k}$  vector ( $\theta_{Be} \approx 0^\circ$ ), resulting in a moderate impact compared with the maximum impact level which requires  $\theta_{Be} = 90^\circ$ .

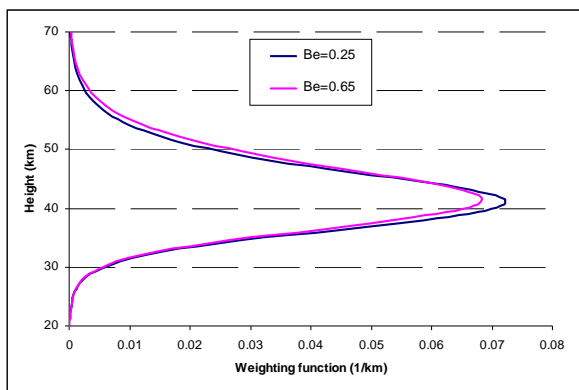


Figure 1. Weighting function of AMSU-A channel 14, calculated using the US76 standard atmospheric temperature profile at  $Be=0.23$  and  $0.65$  in Gauss with  $\cos(\theta_{Be})=0$  for the  $V'$  polarization component.

#### Simulated $T_b(\text{Zeeman}) - T_b(\text{no Zeeman})$ for AMSU-A channel 14

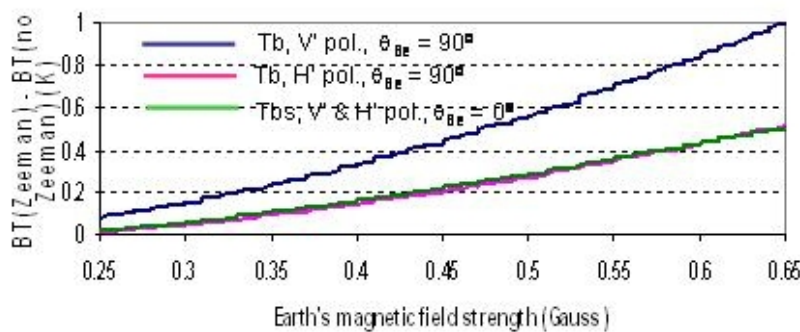


Figure 2. Differences of simulated brightness temperatures (BT) between the models with and without the Zeeman effect.

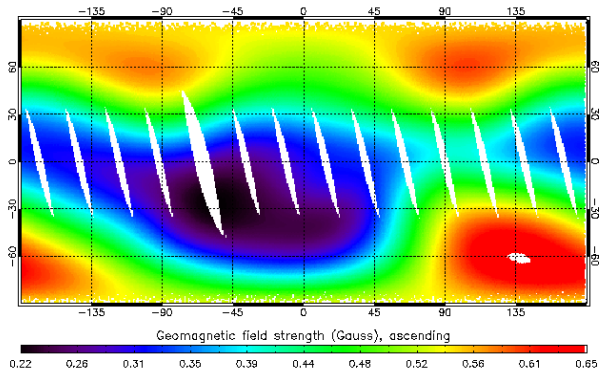


Figure 3A, Earth magnetic field strength  $B_e$  at the pixels of AMSU-A ascending orbits, calculated using the 10<sup>th</sup> International Geomagnetic Reference Field (IGRF) model and the parameters in the 1B data stream.

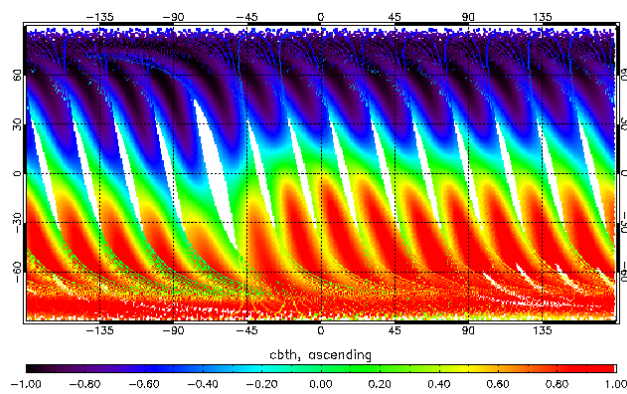


Figure 3B, The  $\cos(\theta_{Be})$  field, i.e. the cosine of the angle between the Earth magnetic field and the wave propagation direction  $\mathbf{k}$  at the pixels of AMSU-A ascending orbits, calculated using the 10<sup>th</sup> International Geomagnetic Reference Field (IGRF) model and the parameters in the 1B data stream.

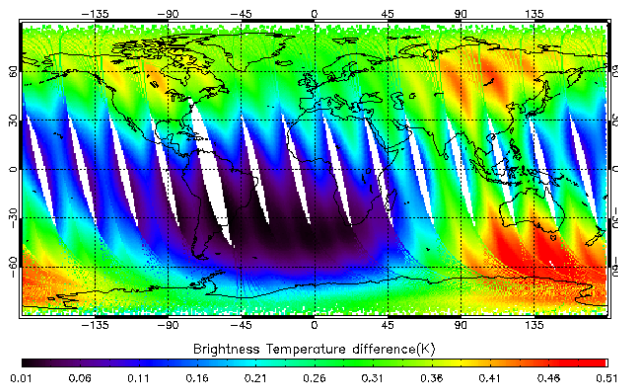


Figure 3C. Differences of the simulated brightness temperatures between the models with and without the inclusion of the Zeeman effect using the data shown in Figure 3A and 3B and the US76 temperature profile, which is applied globally.

## Fast radiative transfer models with the inclusion of Zeeman effect

### Line-by-line base model

The fast RT model is based on the line-by-line (LBL) model Rosenkranz88 (Rosenkranz and Staelin, 1988), which uses a circular polarization basis. The LBL model solves the radiative transfer problem for the brightness temperature coherency matrix,

$$T_b = \begin{bmatrix} T_{b11} & T_{b12} \\ T_{b12}^* & T_{b22} \end{bmatrix}, \quad (1)$$

where  $T_{b11}$  is the component of the right circular polarization,  $T_{b22}$  is the left circular polarization and  $T_{b12}$  is the coherency (the symbol \* represents complex conjugate). The solution of the radiative transfer is given in a numerical form as

$$T_b = \sum_{k=1}^N (P_{k-1} P_{k-1}^+ - P_k P_k^+) T_{a,k}, \quad (2)$$

where

$$P_0 = I, \quad P_k = P_{k-1} \exp(-G_k \Delta z_k), \quad (3)$$

$G_k$  is the complex propagation matrix,  $T_{a,k}$  is the temperature of the  $k^{\text{th}}$  layer,  $I$  is a unit matrix and  $\Delta z_k$  is the thickness of the  $k^{\text{th}}$  layer.

On a linear polarization basis, such as the one used for AMSU-A, the element  $T_{b11}$  in (1) is the brightness temperature with polarization along the  $\mathbf{v}'$  axis in the coordinates system shown in Figure 4, in which the three vectors  $\mathbf{v}'$ ,  $\mathbf{h}'$ , and  $\mathbf{k}$  form a right-handed orthogonal triad, with  $\mathbf{k}$  points to the propagation direction and the  $(\mathbf{v}', \mathbf{k})$  plane contains the earth's magnetic field vector  $\mathbf{Be}$ . It follows that the element  $T_{b22}$  is the component with polarization along the  $\mathbf{h}'$  axis and the off-diagonal elements are the corresponding coherency. The RT solution of brightness temperature matrix with a linear polarization basis can be obtained from the solution on the circular polarization basis through a component transformation and is given by

$$T_{b\_linear} = C T_{b\_circular} C^{-1}, \quad (4)$$

where

$$C = \frac{1}{\sqrt{2}} \begin{bmatrix} 1 & 1 \\ -i & i \end{bmatrix}. \quad (5)$$

AMSU-A channel 14 receives linearly polarized radiation whose polarization varies with scan angle  $\theta_s$  from nadir. It is therefore necessary to transform the brightness temperature components defined in the coordinates shown in Figure 4 into a new coordinates system with the vertical and horizontal polarization defined in a usual way as shown in Figure 5. The result is (Stogryn, 1989),

$$\begin{aligned} T_{b,v} &= \cos^2 \phi_{Be} T_{b,v'} + \sin^2 \phi_{Be} T_{b,h'} - 2 \sin \phi_{Be} \cos \phi_{Be} \text{Re} T_{b,v'h'} \\ T_{b,h} &= \sin^2 \phi_{Be} T_{b,v'} + \cos^2 \phi_{Be} T_{b,h'} + 2 \sin \phi_{Be} \cos \phi_{Be} \text{Re} T_{b,v'h'} \\ T_{b,vh} &= \sin \phi_{Be} \cos \phi_{Be} (T_{b,v'} - T_{b,h'}) + \cos^2 \phi_{Be} T_{b,v'h'} - \sin^2 \phi_{Be} T_{b,v'h'}^* \end{aligned}, \quad (6)$$

where  $\text{Re}()$  is a function for taking the real part of the input variable and the other symbols are defined in Figure 5.

For AMSU-A channel 14, the third terms in the first two equations are not important (well below the 0.1 K level) and thus can be neglected. The brightness temperature that is measured by this channel is thus given by

$$T_b = \sin^2(\theta_s) T_{b,v} + \cos^2(\theta_s) T_{b,h}. \quad (7)$$

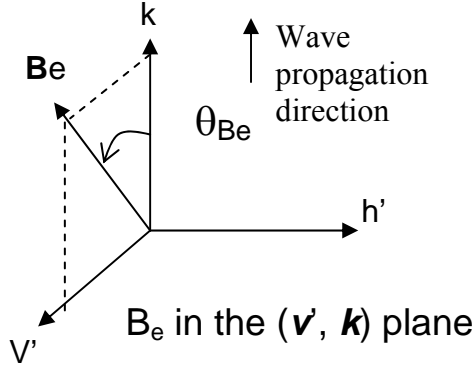


Figure 4. Coordinates with the three vectors  $\mathbf{v}'$ ,  $\mathbf{h}'$ , and  $\mathbf{k}$  forming a right-handed orthogonal triad.

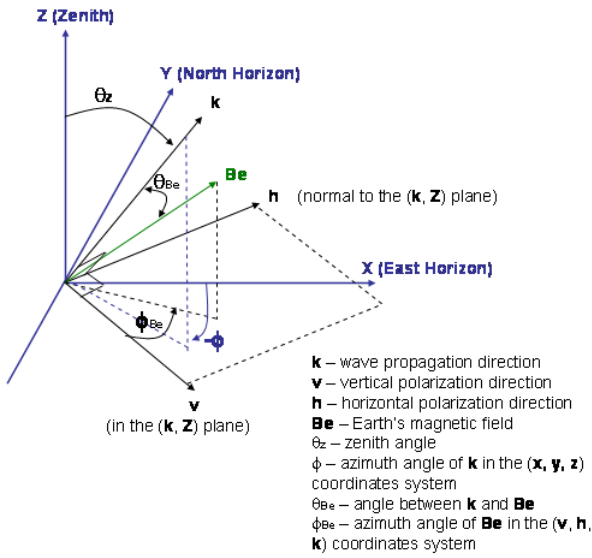


Figure 5. The AMSU-A oriented coordinate system.

### Fast RT model

For an atmosphere vertically divided into  $n+1$  levels from the top of the atmosphere (TOA) to the Earth's surface, the solution for a brightness temperature component with a polarization  $p$  at frequency  $\nu$  may be expressed as

$$T_{b,\nu,p} = \sum_{k=1}^N (\tau_{\nu,k-1,p} - \tau_{\nu,k,p}) T_{a,k}, \quad (8)$$

where  $\tau_{\nu,k,p}$  is an apparent transmittance from level  $k$  to TOA, which was computed using Rosenkranz88, and  $T_{a,k}$  is the mean temperature of the layer between levels  $k-1$  and  $k$ . By averaging both sides of (8) over the channel's passbands we obtain the equation for the passband-averaged brightness temperature,

$$T_{b,ch,p} = \sum_{k=1}^N (\tau_{ch,k-1,p} - \tau_{ch,k,p}) T_{a,k}, \quad (9)$$

where  $\tau_{ch,k,p}$  is the passband-averaged (channel) transmittance. On a linear polarization basis, the transmittance in general depends on geomagnetic field strength  $Be$ , the angle  $\theta_{Be}$  between the magnetic field and wave propagation direction, the azimuth angle  $\phi_{Be}$  (see Figure 5) and air

temperature. However, the  $\varphi_{Be}$  dependence can be first ignored in the transmittance calculation by computing the transmittance in the special coordinates shown in Figure 4 ( $\varphi_{Be}=0$ ). Then, the radiance at an arbitrary  $\varphi_{Be}$  value can be obtained by applying Equation 6.

A linear equation is developed to predict the  $k^{\text{th}}$  layer optical depth  $\sigma_k$  (for the convenience the symbol  $p$  for polarization is dropped),

$$\hat{\sigma}_k = c_{k,0} + \sum_{j=1}^m c_{k,j} x_{k,j}, \quad (10)$$

where  $c_{k,j}$  are coefficients and  $x_{k,j}$  are predictors. With the optical depth profile, the channel transmittances at a zenith angle  $\theta_z$  are then calculated as

$$\hat{\tau}_{ch,k} = \exp\left(-\sum_{i=1}^k \hat{\sigma}_i / \cos(\theta_z)\right), \quad (11)$$

The coefficients  $c_{k,j}$  are obtained through regression. In the regression (training) process, the channel transmittances  $\tau_{ch,k}$  are calculated from a set of diversified atmospheric profiles. The transmittances are then converted to the optical depth  $\sigma_k$  as

$$\sigma_k = \ln(\tau_{ch,k-1} / \tau_{ch,k}) \cos(\theta_z), \quad (12)$$

which is the predictand in the training (dependent) data set. The UMBC 48 profile set (Strow et al., 2003) was adopted and interpolated on the specified levels. The training data set was prepared at the zenith angles corresponding to air masses 1, 1.25, 1.5, 1.75, 2 and 2.5 with eleven points on  $Be$  ( $20 \leq B \leq 70 \mu\text{T}$ ) and 11 points on  $\cos(\theta_{Be})$ . The predictors were configured based in part on the radiance characteristics and in part on trial and error. Table 1 lists the predictors used for the fast RT models.

The fitting error for AMSU-A channel 14 is shown in Figure 6, plotted as a function of the top level set in the fast model (the top level for LBL model is fixed). The fitting error is about 0.035 K for the model with the top level set above 0.02 hPa level.

Table 1. Predictors.  $\psi = 300./T_a$ ,  $T_a$  - air temperature;  $Be$  – geomagnetic field strength;  $\theta_{Be}$  – angle between the geomagnetic field and wave propagation direction;  $\theta_z$  - sensor's zenith angle.

AMSU-A channel 14 Predictors
$\psi, \psi^2 \secant(\theta_z), \cos^2(\theta_{Be}), Be \secant(\theta_z), Be^3, \cos^2(\theta_{Be}) Be^2 \secant(\theta_z)$

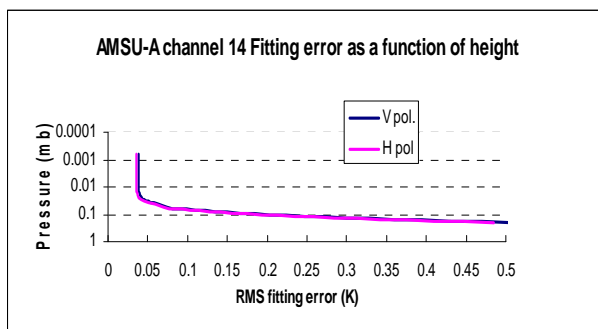


Figure 6. Fitting errors as a function of top pressure level set in the fast model for AMSU-A channel 14.

## Implementation issues

### Handling polarization

As described in the previous section, the AMSU-A Zeeman model requires computations of transmittances for two orthogonal polarizations. This requirement may not be consistent with the model into which the fast Zeeman model is to be implemented, such as the CRTM model (Han et al., 2006), which computes only one transmittance component. To simplify the implementation, polarization may be ignored in the sense that only the following averaged transmittance is predicted,  $\tau = 0.5(\tau_v + \tau_h)$ , (13)

where  $\tau_v$  and  $\tau_h$  are transmittances of the two orthogonal polarizations. This is equivalent to setting the weights of the two brightness temperature components in Eq. (7) to a value of 0.5. With this approach the transmittance calculation and RT integration for this channel can be treated in the same way as the other AMSU channels. It appears that the approach of using the averaged transmittance profile does not significantly degrade the model accuracy (errors in brightness temperature are about 0.1 K or less, depending on the geophysical location and sensor scan angle).

### Obtaining the required input parameters from 1B data set

The AMSU-A 1B data stream does not include the parameters  $Be$ ,  $\cos(\varphi_{Be})$  and  $\cos(\theta_{Be})$ , but they can be derived from the data provided. The following is the steps to compute the parameters.

(a) Compute the magnetic field vector  $Be$  using a lookup table (LUT), which contains pre-computed  $Be$  vectors (a snapshot of the field at a certain date and time) on the grid points of the latitude and longitude with a 2x2 degree grid size. The variation of the vector field with time is less than 2 % and is not important for this channel.

(b) Compute the sensor azimuth angle  $\varphi_{sat}$ , defined here is the angle on the local horizontal plane from the East to the projected line of the  $k$  vector, positive towards North. The 1B data stream provides a relative sensor azimuth angle  $\varphi_r$ , relative to the azimuth angle  $\varphi_{sun}$  of the Sun (see Figure 7), which is not included in the data stream. It is therefore necessary to compute  $\varphi_{sun}$  using the date and time information in the data stream. The sensor's absolute azimuth angle is then computed as

$$\varphi_{sat} = 90 - (\varphi_r + \varphi_{sun}). \quad (14)$$

(c) Compute  $k$  from  $\theta_z$  (sensor's zenith angle) and  $\varphi_{sat}$ .

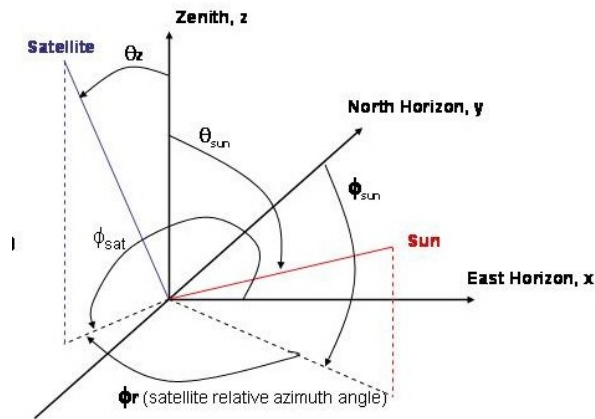
(d) Compute  $\cos(\theta_{Be})$  and  $\cos(\varphi_{Be})$ , as

$$\cos(\theta_{Be}) = Be \bullet k / |Be|$$

and

$$\cos(\varphi_{Be}) = Be_v / Be_p$$

where  $Be_v$  is the component of  $Be$  on the axis of the vertical polarization V (see Figure 5) and  $Be_p$  is the component of  $Be$  projected on the plane containing the V and H vectors.



$\phi_r$  – satellite relative azimuth angle the arrow indicate the angle taking the positive value  
 $\phi_{sun}$  – sun azimuth angle from North (East positive)  
 $\theta_{sun}$  – sun zenith angle  
 $\theta_z$  – satellite zenith angle

Figure 7. The relationship between the relative sensor azimuth angle and the azimuth angle of the Sun.

## Summary

The Zeeman-splitting can have an effect up to 0.5 K in brightness temperature on AMSU-A channel 14, depending on the pixel locations and the observation direction relative to the Earth magnetic field vector. To take the effect into account, a fast radiative transfer model has been developed for applications requiring rapid radiance calculations. The fast model is trained with the LBL mode Rosenkranz88 and has a RMS difference of less than 0.1 K compared with the LBL base model. To simplify the implementation, polarization may be ignored with a small reduction of the model accuracy (up to 0.1 K).

## References

- Fleming, E.L., S. Chandra, M. R. Shoerberl, and J. J. Barnett (1988), Monthly mean global climatology of temperature, wind, geopotential height and pressure for 0-120 km, *National Aeronautics and Space Administration*, Technical Memorandum 100697, Washington, D.C..
- Han, Y., F. Weng, Q. Liu and P. van Delst (2007), A Fast Radiative Transfer Model for SSMIS Upper-atmosphere Sounding Channels, *J. Geophys. Res.*, **112**, D1121, doi:10.1029/2006JD008208.
- Han, Y., P. van Delst, Q. Liu, F. Weng, B. Yan, R. Treadon, J. Derber (2006), Community Radiative Transfer Model (CRTM) – Version 1, *NOAA NESDIS Technical Report 122*.
- McMillin, L. M., L. J. Crone, M. D. Goldberg, and T. J. Kleespies (1995), Atmospheric transmittance of an absorbing gas. 4. OPTRAN: a computationally fast and accurate transmittance model for absorbing gases with fixed and variable mixing ratios at variable viewing angles, *Appl. Opt.* **34**, 6269 - 6274.
- Rosenkranz, P. W. and D. H. Staelin (1988), Polarized thermal microwave emission from oxygen in the mesosphere, *Radio Science*, **23**, 721-729.



Russell, J. M., III, M. G. Mlynczak, L. L. Gordley, J. Tansock, and R. Esplin (1999), An overview of the SABER experiment and preliminary calibration results, presented at the 44<sup>th</sup> Annual Meeting, Int. Soc. For Opt. Eng., Denver, Colo., 18-23 July 1999.

Stogryn, A. (1989), The magnetic field dependence of brightness temperature at frequencies near the O<sub>2</sub> microwave absorption lines, *IEEE Transactions on Geoscience and Remote Sensing*, 27, 279-289.

Strow L.L., S. E. Hannon, S. D. Souza-Machado, H. E. Mottler, and D. Tobin (2003), An overview of the AIRS radiative transfer model," *IEEE Transactions on Geoscience and Remote Sensing*, 41, 303 – 313.